

## Article

# Estimation of the Effects of CO<sub>2</sub> and Temperature on the Swelling of PS-CO<sub>2</sub> Mixtures at Supercritical Conditions on Rheological Testing

César Miguel Ibarra-Garza <sup>1</sup>, Cecilia D. Treviño-Quintanilla <sup>2,3,\*</sup> and Jaime Bonilla-Ríos <sup>1,\*</sup><sup>1</sup> School of Engineering and Science, Tecnológico de Monterrey, Monterrey 64849, Mexico<sup>2</sup> Institute of Advanced Materials for Sustainable Manufacturing, Tecnológico de Monterrey, Queretaro 76146, Mexico<sup>3</sup> Laboratorio Nacional de Manufactura Aditiva y Digital (MADIT), Autopista al Aeropuerto, Km. 9.5, Calle Alianza Norte 100, Apodaca 66629, Mexico

\* Correspondence: cdtrevino@tec.mx (C.D.T.-Q.); jbonilla@tec.mx (J.B.-R.)

**Abstract:** The use of supercritical CO<sub>2</sub> as a blowing agent for polymeric foams instead of traditional blowing agents has been a trend in recent years. To achieve the final desired properties of the polymeric foams, the rheological behavior of the material needs to be reliable. The polymer swelling in the samples for rheological testing affects the results of the viscoelastic properties of the material. This study proposes a new testing methodology to control the accuracy and repeatability of the rheological characterization for PS-SCO<sub>2</sub> samples. To develop this methodology, three polystyrene resins with different molecular weight distribution were studied at three temperatures (170, 185 and 200 °C) and three pressures (0.1 MPa, 6.89 MPa and 13.78 MPa). The CO<sub>2</sub> concentration was estimated and used in the Sanchez–Lacombe Equation of State (SLEOS) to determine the polymer swelling, as it affects the dimensions of specimens tested in high-pressure rheometers. The correction factors provided a consistent trend in the viscosity with respect to temperature and a decrease of up to 50% in the standard deviation. The results of this study are crucial for an accurate measurement of viscoelastic properties by parallel-plate rheometry.

**Keywords:** polystyrene; carbon dioxide; swelling; viscoelasticity

**Citation:** Ibarra-Garza, C.M.; Treviño-Quintanilla, C.D.; Bonilla-Ríos, J. Estimation of the Effects of CO<sub>2</sub> and Temperature on the Swelling of PS-CO<sub>2</sub> Mixtures at Supercritical Conditions on Rheological Testing. *Polymers* **2022**, *14*, 3490. <https://doi.org/10.3390/polym14173490>

Academic Editor: Francisco Javier Navarro

Received: 25 July 2022

Accepted: 17 August 2022

Published: 26 August 2022

**Publisher's Note:** MDPI stays neutral with regard to jurisdictional claims in published maps and institutional affiliations.



**Copyright:** © 2022 by the authors. Licensee MDPI, Basel, Switzerland. This article is an open access article distributed under the terms and conditions of the Creative Commons Attribution (CC BY) license (<https://creativecommons.org/licenses/by/4.0/>).

## 1. Introduction

Polymeric foams are produced by adding a blowing agent into a molten polymer. These foams can be found in airplanes and automotive parts, as acoustic or thermal insulators for construction or appliances and as varieties of cushioning for furniture or packaging to avoid product damage. One of the most important methods for producing polymeric foams is the extrusion process that uses supercritical fluids (SCFs) as blowing agents.

The effect of SCFs has been investigated in a variety of polymers: polyethylene, polypropylene, and polystyrene, among others. Sc-CO<sub>2</sub> has received special attention, as it is environmentally friendly and can be easily removed by depressurization, reducing, for instance, the cost and processing time compared to other methods that require drying or solvent removal. Another benefit of using Sc-CO<sub>2</sub> for polymer foaming is the polymers' plasticization at low temperatures, preventing thermal degradation of resins during processing.

Understanding the mixing of supercritical fluids in a polymer matrix requires accurate measurements of viscoelastic properties under high pressures and temperatures. For high-pressure rheology, different geometries can be adapted for drag and pressure flows. The most-used rheometer consists of a slit-die rheometer first adapted by Han [1]. This configuration was later used by Han and Ma, Royer et al., and Lee et al. Others have used a Couette rheometer [2] and a parallel plate [2,3]. However, available equipment consisting in a parallel-plate rheometer inside a pressure cell incurs errors related to configuration [4,5].

It has been proved that for any rheological measurements, the errors can increase up to 7% when testing with samples with a smaller diameter than the plate's (underfilling) [6] and up to 30% when overfilling happens [4]. Therefore, it is important to know in advance the corrections for volume, thermal expansion and swelling to adjust the specimen dimensions before the rheological test is conducted. Different authors were focused on studying the shrinkage problem in polymer foams with SCFs [7] or characterizing the thermal properties of the foams [8] without developing a method to reduce the measurement error by the rheometers.

This study developed a testing methodology to provide accuracy and repeatability of rheology testing using a parallel-plate rheometer in a pressure cell, supported by the Sanchez-Lacombe Equation of State (SLEOS) [9]. The study covers a wide range of operating conditions using temperatures from 170 to 200 °C and pressures of 0.01, 6.89 and 13.78 MPa of CO<sub>2</sub> for later use in the parallel-plate rheometry.

## 2. Materials and Methods

### 2.1. Materials

Standard characterization methods were performed for each sample, such as gel permeation chromatography (GPC) for molecular weight distribution (MWD) data from Malvern Instruments, Houston, TX, USA. Also differential scanning calorimetry (DSC) for the glass transition temperature valuation using a DSC from TA Instruments, New Castle, DE, USA.

Three polystyrene resins with different molecular weight distribution (MWD) were used in this study (Table 1). These were provided by Total Petrochemicals & Refining USA, Inc., Deer Park, TX, USA.

**Table 1.** Molecular weight distribution (MWD) parameters and the glass transition temperatures ( $T_g$ ) for all the PS resins.

Resin ID	$M_n$	$M_w$	$M_z$	Polydispersity	Peak $M_w$	$T_g$ (°C)
A	124,756	317,113	521,655	2.5	298,925	106.10
B	85,810	252,217	442,775	2.9	247,823	101.88
C	103,405	257,557	48,2252	2.5	224,748	106.34

Here,  $M_n$  is the number average molecular weight,  $M_w$  is the average molecular weight,  $M_z$  is the third moment of the MWD,  $M_w/M_n$  is the polydispersity index, and the Peak  $M_w$  is the highest peak of the  $M_w$  curve. This Peak  $M_w$  is usually extracted for very narrow distributions of  $M_w$  in polymers.

### 2.2. Sample Preparation

13.4 and 14.6 mm diameter round samples with 1.5 mm of thickness were fabricated using a hydraulic press, Carver Inc, Wabash, IN, USA., molded at 204 °C in two cycles. First, the resins were stabilized with 2% BHT (butylhydroxytoluene) by Sigma-Aldrich, Burlington, MA, USA. The first cycle consisted in 5 min of pressing at 20.7 MPa, followed by a second cycle of 5 min at 413.7 MPa.

### 2.3. Oscillatory Rheometry

High-pressure rheology data were obtained from strain-controlled frequency sweeps data using an Anton Paar SmartPave MCR101, Graz, Austria, rheometer equipped with a pressure cell with a 20 mm parallel-plate configuration and 1 mm gap at 170 °C, 185 °C and 200 °C and two pressures, 6.89 MPa and 13.78 MPa, in addition to atmospheric pressure (0.10 MPa). The strain was fixed at 10%.

Figure 1 shows the experimental setup consisting of two Teledyne ISCO syringe pumps by Lincoln, NE, USA, with a D-series pump controller. A CO<sub>2</sub> cylinder is connected to syringe pump B, which is responsible for filling up pump A. Two check valves help the

pressurization process for both pumps. After pressurization, a manual gate valve is opened to pressurize the cell (already sealed and loaded with a sample) while pump A is running.

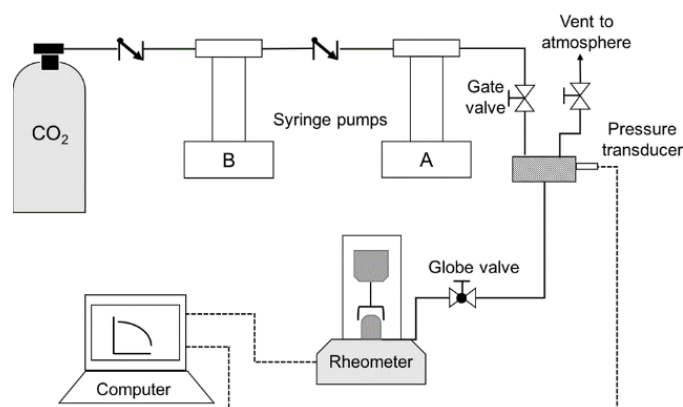


**Figure 1.** Schematic of the experimental setup: two syringe pumps used to pressurize with CO<sub>2</sub> the cell of the rheometer already sealed and loaded with a PS sample.

To obtain accurate viscosity data from the rheometer, an experimental methodology was developed. This methodology ensures the repeatability of the tests. As seen in the rheometer’s schematic (Figure 1), the equipment design does not allow manipulation of the sample once placed in testing position. The first step is to prepare the samples and gauge the gap manually to assure the dimensions, and then defining the time of measurements and solubility is required. Under these considerations, the swelling and the actual radius were calculated so that viscosity data could be adjusted. The complete methodology of the experimental process is seen in Figure 2. This methodology’s repeatability is affected by the five elements seen in Figure 2: sample dimensions, gap, sample deformations, degradation and measurement time. This study proposed a setup to reduce the errors in the experimental data controlling these five elements.

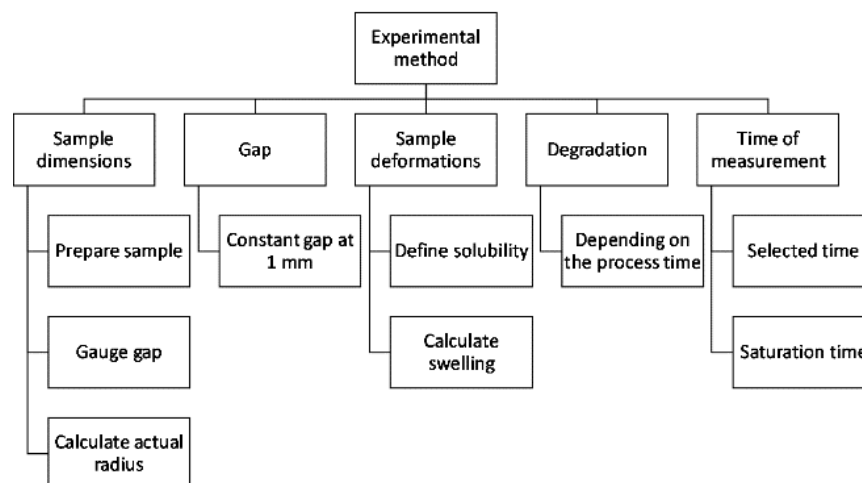


**Figure 2.** Experimental methodology for this study.

#### 2.4. Volumetric Thermal Expansion

In order to have a gap control in the measurements, the volumetric thermal expansion of the samples was measured. All the samples were heated and deformed for 10 min at a fixed temperature. Then, the pressure was opened, and the final diameter and thickness were measured using a Vernier caliper.

The volumetric thermal expansion coefficient ( $\beta_T$ ) was calculated using Equation (1):

$$V_F = V_0(1 + \beta_T \Delta T) \tag{1}$$

where  $V_0$  and  $V_F$  are the initial and final volume, respectively, and  $\Delta T$  is the difference between initial ( $T_0$ ) and final temperature ( $T_F$ ).

### 2.5. CO<sub>2</sub> Concentration

In order to use the SLEOS, first, defining the solubility of CO<sub>2</sub> in PS is required. Henry constant works well for modeling this system; therefore, Equation (2), which was reported by Sato et al. [10], was used for PS + CO<sub>2</sub>:

$$\ln(k_p) = 6.400 + 2.537 \left( \frac{T_c}{T} \right)^2 \quad (2)$$

where  $k_p$  is the Henry constant (kg. MPa/cm<sup>3</sup> STP),  $T_c$  is the CO<sub>2</sub> critical temperature (304.2 K) [11], and  $T$  is the temperature of the system. This equation has been proven to correlate experimental Henry constant within average relative deviations of 2.5% for this system [10].

### 2.6. Swelling

Thermodynamic equations of states (EOS) are needed to model the interactions between the polymer and SCFs to describe the system state in terms of pressure and temperature, which will determine solubility, the density of the mixture and even phase stability.

The SLEOS [12] is the most used for polymer-SCF systems, and its effectiveness has been proved for describing different polymer-SCF systems accurately [2,10,13–15]. It can be used for calculating the density of a mixture in correlation with the absorption of a gas into the polymer, the fractional free volume, swelling, and phase stability. Therefore, SLEOS is useful in high-pressure rheology because it indirectly considers the plasticization effect of changes in free volume as the gas dissolves in the polymer system.

SLEOS is based on the chemical potential of a system (3) at equilibrium (4), given by:

$$\mu = rNe^* \left[ -\tilde{\rho} + \tilde{P}\tilde{v} + \tilde{T}\tilde{v} \left[ (1 - \tilde{\rho}) \ln(1 - \tilde{\rho}) + \frac{\tilde{\rho}}{r} \ln \tilde{\rho} \right] \right] \quad (3)$$

$$\tilde{\rho}^2 + \tilde{P} + \tilde{T} \left[ \ln(1 - \tilde{\rho}) + \left( 1 - \frac{1}{r} \right) \tilde{\rho} \right] = 0 \quad (4)$$

where  $N$  is the total number of moles;  $r$  is the number of lattices occupied by a molecule;  $\tilde{\rho}$ ,  $\tilde{T}$ ,  $\tilde{v}$  and  $\tilde{P}$  are reduced density, temperature, volume and pressure, respectively, according to their characteristic values (superscript \*), and  $\epsilon^*$  is the characteristic energy of interaction per mer, that is:

$$\tilde{T} = T/T^* \quad (5)$$

$$\tilde{P} = P/P^* \quad (6)$$

$$\tilde{\rho} = \rho/\rho^* \quad (7)$$

$$\tilde{v} = v/v^* \quad (8)$$

Characteristic parameters for pure components are determined by correlating empirical PVT data with Equation 4. Thus, measurements of solubility and swelling at equilibrium are required. Detailed procedures for determining characteristic parameters can be found elsewhere [9,16]. These procedures can be carried out using experimental setups for the pressure decay method or gravimetric method [17,18].

The SLEOS works with a dimensionless binary interaction parameter ( $k_{12}$ ) that considers the deviations caused by pressure, and it is considered in the calculation of the characteristic pressure of the mixture ( $P^*$ ), which accounts for the cohesiveness of the fluid [12]. According to findings from Sato et al. [19,20], the binary interaction parameter can be modeled as temperature-dependent. Therefore, values from Sato et al. were used to

predict the binary interaction parameter for the desired temperatures via a linear regression, resulting in Equation (9):

$$k_{12} = -0.0011T + 0.330 \quad (9)$$

Other values for the interaction parameter can be found elsewhere [2,19].

## 2.7. CO<sub>2</sub> and PS Properties

The density for both the PS and CO<sub>2</sub> was estimated according to the following models.

### 2.7.1. Carbon Dioxide Properties

Density for CO<sub>2</sub> at supercritical state was calculated using Peng–Robinson (PR) EOS [21]:

$$P = \frac{R_g T}{V - b_{PR}} - \frac{a(T)}{V(V + b_{PR}) + b_{PR}(V - b_{PR})} \quad (10)$$

where:

$$a(T) = \frac{0.45724 R_g^2 T_c^2}{P_c} * \alpha(T) \quad (11)$$

$$b_{PR} = 0.07780 R_g T_c / P_c \quad (12)$$

$$\alpha(T) = \left[ 1 + k(1 - T_r^{0.5}) \right]^2 \quad (13)$$

$$k = 0.3746 + 1.54226 \omega_a - 0.26992 \omega_a^2 \quad (14)$$

where  $P$  is pressure,  $R_G$  is the gas constant,  $T$  is temperature,  $a$ ,  $b_{PR}$  and  $k$  are the Peng–Robinson parameters,  $V$  is volume,  $T_c$  is the critical temperature,  $P_c$  is the critical pressure,  $\omega_a$  is the acentric factor, and  $T_r$  is the reduced temperature.

### 2.7.2. Polystyrene Properties

For PS, there are no equations to exactly calculate the density; however, there are some models reported by Mark [22] that show agreement with experimental data within a range of operating conditions. Equation (15) can estimate the PS density for different temperatures at atmospheric pressure:

$$\rho = a_0 + a_1 T + a_2 T^2 \quad (15)$$

where  $a_0$ ,  $a_1$  and  $a_2$  are constants that can be found in Table 2, depending on the temperature range and the reference by which this information was obtained.

**Table 2.** Constants used in Equation (15) to calculate the density of PS at atmospheric pressure.

$a_0$	$a_1$	$a_2$	$T_{\min}$ – $T_{\max}$	Ref.
1.0865	$-6.19 \times 10^{-4}$	$1.36 \times 10^{-7}$	100–200 °C	[23]
1.067	$-5.02 \times 10^{-4}$	$1.35 \times 10^{-7}$	79–320 °C	[24]

On the other hand, to calculate densities as a function of temperature and pressure, the following model is reported [22]:

$$\rho(P, T) = \frac{\rho(0, T)}{1 - C \cdot \ln\left(1 + \frac{P}{B(T)}\right)} \quad (16)$$

$$B(T) = b_0 e^{-b_1 T} \quad (17)$$

where  $\rho(0, T)$  represents the density at atmospheric pressure and reference temperature, and  $b_0$  and  $b_1$  are constants shown in Table 3, at desired operating conditions.

**Table 3.** Constants used in Equations (16) and (17) to calculate density of PS as a function of temperature and pressure.

$b_0$	$b_1$	C	$T_{\min}-T_{\max}$ (°C)	$P_{\min}-P_{\max}$ (bar)
2435	0.00414	0.09	115–249	0–2000
2521	0.00408	0.09	79–320	0–1800

### 3. Results and Discussion

Since the presence of CO<sub>2</sub> changes the material properties and dimensions, the amount of CO<sub>2</sub> dissolved into the polymer and the resulting swelling are needed at each testing condition for the testing to be accurate. In addition, thermal expansion must be considered to validate testing results, as samples' dimensions are affected by CO<sub>2</sub> concentration and temperature.

#### 3.1. Volumetric Thermal Expansion

Polymer samples need to cover the rheometer's plate completely to avoid errors due to underfilling or excess on the edges. The results of the calculated volumetric expansion using Equation (1) are shown in Table 4.

**Table 4.** Calculated values of volumetric thermal expansion coefficient ( $\beta_T$ ) for PS.

$T_0$ (°C)	$T_F$ (°C)	$V_0$ (mm <sup>3</sup> )	$V_F$ (mm <sup>3</sup> )	$\beta_T$ (°C <sup>-1</sup> )
25	185	176.84	206.08	$1.03 \times 10^{-3}$
25	185	178.69	247.45	$2.40 \times 10^{-3}$
25	185	177.95	212.88	$1.23 \times 10^{-3}$
25	200	170.48	247.73	$2.59 \times 10^{-3}$
25	200	207.00	277.74	$1.95 \times 10^{-3}$

Here,  $T_0$  is initial temperature,  $T_F$  is the final temperature,  $V_0$  is the initial volume of the samples,  $V_F$  is the final volume of the samples, and  $\beta_T$  is the volumetric thermal expansion coefficient.

An average value of  $1.8 \times 10^{-3}/^\circ\text{C}$  was used as the volumetric thermal expansion coefficient. Validation of this empirical value was performed with data from the literature. Averaged volumetric thermal expansion coefficients showed agreement with data reported by Mark [22]

#### 3.2. Solubility of CO<sub>2</sub>

Using the Henry constant, the solubility (g CO<sub>2</sub>/g PS) for each pair of operating conditions was calculated as seen in Table 5.

**Table 5.** Solubilities for CO<sub>2</sub> in PS at various temperatures and pressures.

Pressure (MPa)	Temperature (K)	Solubility (g CO <sub>2</sub> /g PS)
6.89	443.15	0.027
	458.15	0.025
	473.15	0.023
13.78	443.15	0.053
	458.15	0.049
	473.15	0.046

The predicted values for the binary interaction ( $k_{12}$ ) parameters for PS and CO<sub>2</sub> mixtures obtained by linear regression (Equation (9)) are shown in Table 6.

**Table 6.** Predicted binary interaction parameters for PS + CO<sub>2</sub> at different temperatures using Equation (9).

Temperature (K)	k <sub>12</sub>
443.15	−0.144
458.15	−0.160
473.15	−0.180

To calculate the mixture properties of PS + CO<sub>2</sub> systems, some characteristic parameters are needed. These have been reported in different studies [2,12,13,25], but the ones used for this research are presented in Table 7, reported by Sato et al. [10].

**Table 7.** Characteristic parameters of PS and CO<sub>2</sub> used in SLEOS.

Compound	$\rho^*$ (kg/m <sup>3</sup> )	P* (MPa)	T* (K)
PS	1108	387	739.9
CO <sub>2</sub>	1580	720.3	$208.9 + 0.459 T - 7.56 \times 10^{-4} T^2$

Other inputs for SLEOS, in addition to operating temperature and pressure, are the material's density and molecular weight. For PS, the weight-averaged molecular weight ( $M_w$ ) was taken as the molecular weight.

### 3.3. Materials Properties Estimation

#### 3.3.1. Carbon Dioxide

Tables 8 and 9 present the calculated critical properties and densities of CO<sub>2</sub> using the Peng-Robinson (PR) EOS (Equation (10)) at different temperatures and pressures.

**Table 8.** Critical properties of the CO<sub>2</sub> obtained by PR EOS.

T <sub>C</sub> (K)	P <sub>C</sub> (atm)	$\omega_a$
304.2	72.9	0.224

**Table 9.** Densities of CO<sub>2</sub> at different temperatures and pressures obtained by PR EOS.

Pressure (MPa)	Temperature (K)	Density, $\rho$ (kg/m <sup>3</sup> )
6.89	443.15	90.25
	458.15	86.14
	473.15	82.46
13.78	443.15	193.68
	458.15	182.52
	473.15	172.93

#### 3.3.2. Polystyrene

It can be seen from Tables 2 and 3 that the temperature and pressure ranges in which both sets of constants work are compatible to the ones used in this study; therefore, averages of the results from both sets were calculated and are shown in Table 10.

It is important to mention that it was not possible to measure the real density of each resin due to lack of appropriate equipment, and the values presented in Table 10 were considered the same for the three resins.

**Table 10.** Densities of PS calculated at different temperatures and pressures by using Equations (15–17).

P (MPa)	T (°C)	Average (Models)
		$\rho$ (kg/m <sup>3</sup> )
0.1	170	985.38
	185	977.69
	200	970.07
6.89	170	990.20
	185	982.78
	200	975.42
13.78	170	994.82
	185	987.63
	200	980.52

### 3.4. Swelling

Having the solubility, the interaction parameter and the materials properties, it was possible to use the SLEOS to estimate the swelling. The estimated volumes of the mixture using SLEOS (Equations (3)–(9)) are shown in Table 11. The expected behavior, namely that the higher the temperature and pressure, the higher the CO<sub>2</sub> solubility and, therefore, the higher the swelling, can be verified through the results obtained by SLEOS.

**Table 11.** Swelling ratios for PS + CO<sub>2</sub> at various temperatures and pressures using SLEOS.

P (MPa)	T (K)	Swelling Ratio
6.89	443.15	1.034
	458.15	1.032
	473.15	1.035
13.78	443.15	1.068
	458.15	1.067
	473.15	1.067

The assumption of a fixed gap of 1 mm impacts the volume and therefore the radius sample. The volume of a cylinder (sample's shape) is defined by:

$$V_{cl} = \pi R^2 H \quad (18)$$

where  $R$  is the sample's radius and  $H$  is the height, in this case equal to or defined by the gap.

In any case, the volume increases due to the thermal expansion and swelling caused by the dissolution of CO<sub>2</sub> in the PS specimen. It has been shown that, on average, the effect for thermal expansion is 87% while the rest is due to swelling when at 6.89 MPa, and the effect is 77% when at 13.78 MPa. Therefore, the effect on the specimen is around 10%, which could affect the results by approximately 52%.

Finally, having estimated the swelling ratio via SLEOS, the real volume can be used to calculate the final sample's radius. Based on this experiment and considering that the thickness is fixed by the plates (gap), the final discs dimensions for each temperature are shown in Table 12.



**Table 12.** Polymer discs dimensions after and during testing with SC-CO<sub>2</sub>.

P (MPa)	T (K)	h <sub>i</sub> (mm)	d <sub>i</sub> (mm)	β <sub>T</sub> (°K <sup>-1</sup> )	Swelling Ratio	H (mm)	d <sub>f</sub> (mm)
6.89	443.15	1.56	14.60	1.8 × 10 <sup>-3</sup>	1.034	1	20.82
	458.15		14.60		1.032		21.02
	473.15		13.40		1.035		19.53
13.78	443.15	1.56	14.60	1.8 × 10 <sup>-3</sup>	1.068	1	21.17
	458.15		14.60		1.067		21.38
	473.15		13.40		1.067		19.82

Here, T is temperature, d<sub>i</sub> is the initial diameter, h<sub>i</sub> is the initial height, β<sub>T</sub> is the volumetric thermal expansion coefficient, H is the gap, and d<sub>f</sub> is the final diameter.

### 3.5. Oscillatory Rheometry

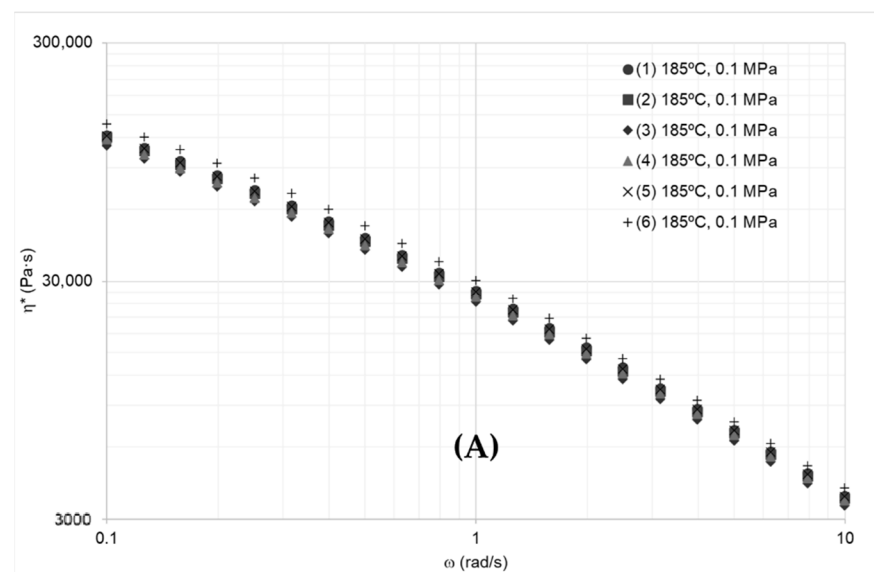
In the case of the parallel-plate rheometer, the complex viscosity (η\*) is affected by the gap and radius as follows:

$$\eta^* = \frac{\tau}{\dot{\gamma}} = \frac{2MH}{\pi\omega R^4} \quad (19)$$

where H is the gap, M is the torque, ω is the frequency, τ is the shear stress, and  $\dot{\gamma}$  is the shear rate.

Results from adjusting the data indicate that the protocol and corrections produced consistent data by reducing the test's standard deviation by at least 52%, as seen in Figure 3.

Another problem solved with data treatment was the correction of the collapsing effect on the complex viscosity curves for all resins, as shown in Figure 4A at high frequencies. This was a major concern, since the expected trend in the complex viscosity was that the higher the temperature, the lower the viscosity. This implied that the effect of the temperature on the viscosity was violated. As the data were processed, introducing the swelling factor, the expected behavior of the complex viscosity was achieved. This correction can be observed in Figure 4B.

**Figure 3.** Cont.

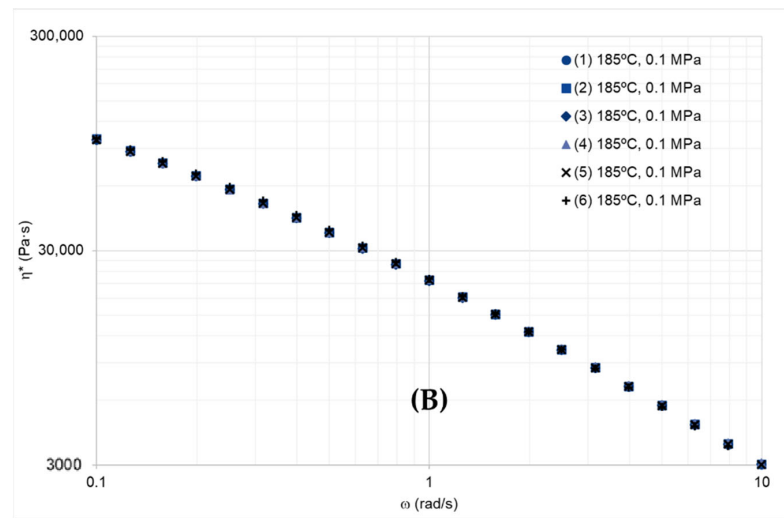


**Figure 3.** (A) Complex viscosity of several samples of Resin A as reported by the instrument (rheometer), (B) the same data recalculated using the actual radius in Equation (19).

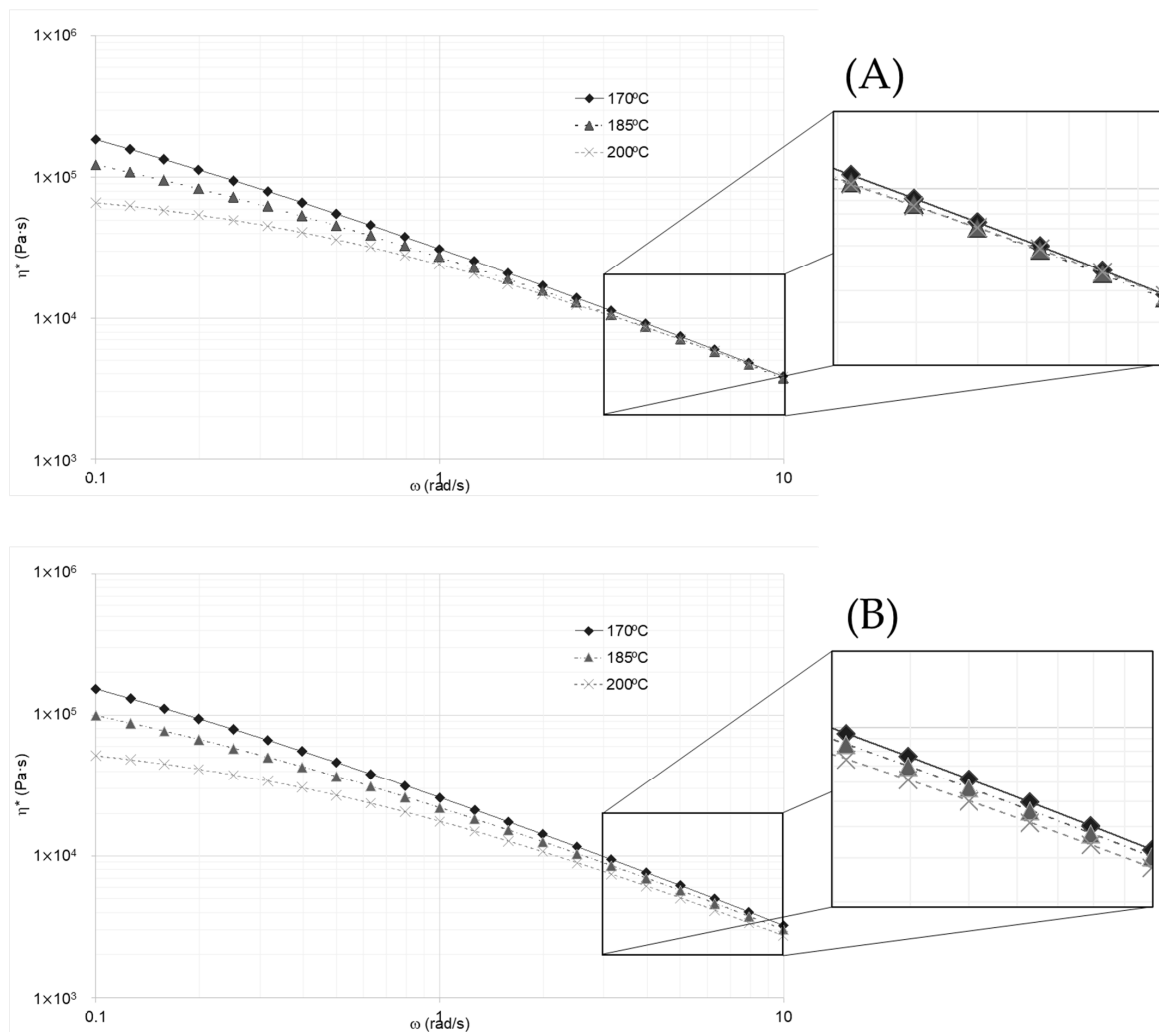


**Figure 4.** (A) Complex viscosity curves for resin A at different temperatures collapsing at high frequencies, (B) adjusted complex viscosity of resin A at different temperatures after correction for swelling, splitting off at high frequencies.

The correlations of solubility using PC-SAFT [26] and PR [21] equations of state were investigated using the results obtained by Arce and Aznar [27] and compared with the ones using the Henry constant and SLEOS in this study. The results using SLEOS to model the mixture of polymers and SCF were accurate. Other EOS were evaluated in order to identify differences between models.

For practicality, the solubility was compared at 458.15 K and both pressures (6.89 MPa and 13.78 MPa). Table 13 shows the comparison of solubility correlations using different equations.

**Table 13.** Comparison of solubility using different EOS: SLEOS, PC-SAFT and PR.

		SLEOS	PC-SAFT	PR	SLEOS vs. PC-SAFT	SLEOS vs. PR
P (MPa)	T (K)	Solubility (g CO <sub>2</sub> / g PS)			% difference	
6.89	458.15	0.025	0.026	0.030	5%	18%
13.78	458.15	0.049	0.054	0.059	9%	18%

The results show that SLEOS has a minor difference from estimations using PC-SAFT; however, differences from PR equation of state are significant, suggesting that PR may not be an appropriate model for PS+CO<sub>2</sub> mixtures. On the other hand, SLEOS and PC-SAFT showed good agreement, so both can be considered as valid models to describe these systems.

#### 4. Conclusions

In order to achieve a correct study of the viscoelastic behavior of polystyrene resins containing supercritical CO<sub>2</sub> for foaming applications, it was necessary to develop an experimental procedure for a parallel-plate rheometer to assure repeatability and reproducibility.

Developed protocol controls variables from the instrument, the material and mixing phenomena. Control of material's variables included mass and volume of the samples, deformations caused by thermal expansion and squeezing the polymer sample (for testing). Results indicate that the protocol offers consistent data by reducing standard deviations by at least 52% and by solving the problem of the collapsing effect of the complex viscosity at different temperatures (Figure 3).

Estimations of swelling ratios were possible using SLEOS. In this model, the binary parameter played an important role for modeling the mixing phenomenon. This study shows the importance of using equations of state to adjust the dimensions of the samples for parallel-plate rheometry for these mixtures.

**Author Contributions:** Conceptualization, J.B.-R.; methodology, C.M.I.-G.; validation, C.M.I.-G. and C.D.T.-Q.; formal analysis, C.M.I.-G., and J.B.-R.; investigation, C.M.I.-G., and C.D.T.-Q.; resources, J.B.-R.; data curation, J.B.-R.; writing—original draft preparation, all.; writing—review and editing, C.D.T.-Q.; visualization, J.B.-R.; supervision, J.B.-R.; project administration, J.B.-R.; funding acquisition, J.B.-R. All authors have read and agreed to the published version of the manuscript.

**Funding:** Provided by Total Petrochemicals and Refining, USA.

**Institutional Review Board Statement:** Not applicable.

**Informed Consent Statement:** Not applicable.

**Data Availability Statement:** The data presented in this study are available on request from the corresponding author.

**Acknowledgments:** The authors gratefully acknowledge the support of Total Petrochemicals and Refining, USA, as well as Jayna Brown, Russel McDonald and Leonardo Cortes for the test performance and support. Grateful acknowledgement also goes to the Consejo Nacional de Ciencia y Tecnología (CONACyT) and Tecnológico de Monterrey in Mexico.

**Conflicts of Interest:** The authors declare no conflict of interest.

## References

1. Han, C.D. Measurement of the Rheological Properties of Polymer Melts with Slit Rheometer. I. Homopolymer Systems. *J. Appl. Polym. Sci.* **1971**, *15*, 2567–2577. [[CrossRef](#)]
2. Wingert, M.J.; Shukla, S.; Koelling, K.W.; Tomasko, D.L.; Lee, L.J. Shear Viscosity of CO<sub>2</sub>-Plasticized Polystyrene under High Static Pressures. *Ind. Eng. Chem. Res.* **2009**, *48*, 5460–5471. [[CrossRef](#)]
3. Handge, U.A.; Altstädt, V. Viscoelastic Properties of Solutions of Polystyrene Melts and Carbon Dioxide: Analysis of a Transient Shear Rheology Approach. *J. Rheol.* **2012**, *56*, 743–766. [[CrossRef](#)]
4. Cardinaels, R.; Reddy, N.K.; Clasen, C. Quantifying the Errors Due to Overfilling for Newtonian Fluids in Rotational Rheometry. *Rheol. Acta* **2019**, *58*, 525–538. [[CrossRef](#)]
5. Kumai, Y.; Suzuki, I.; Tousen, Y.; Kondo, T.; Kayashita, J.; Chiba, T.; Furusho, T.; Takebayashi, J. Reliability in Viscosity Measurement of Thickening Agents for Dysphagia Management: Are Results Obtained by Cone-and-Plate Rheometers Reproducible between Laboratories? *J. Texture Stud.* **2022**, *53*, 315–322. [[CrossRef](#)]
6. Hellström, L.O.; Samaha, M.; Wang, K.; Smits, A.; Hultmark, M. Errors in Parallel-Plate and Cone-Plate Rheometer Measurements Due to Sample Underfill. *Meas. Sci. Technol.* **2015**, *26*, 015301. [[CrossRef](#)]
7. Zhang, H.; Liu, T.; Li, B.; Li, H.; Cao, Z.; Jin, G.; Zhao, L.; Xin, Z. Anti-Shrinking Foaming of Polyethylene with CO<sub>2</sub> as Blowing Agent. *J. Supercrit. Fluids* **2020**, *163*, 104883. [[CrossRef](#)]
8. Yao, S.X.; Lee, P.C.; Park, H.E.; Schadler, L.S. A Novel Method to Characterize Thermal Properties of the Polymer and Gas/Supercritical Fluid Mixture Using Dielectric Measurements. *Polym Test* **2020**, *92*, 106861. [[CrossRef](#)]
9. Sanchez, I.; Lacombe, R. An Elementary Equation of State for Polymer Liquids. *J. Polym. Sci.* **1977**, *15*, 71–75. [[CrossRef](#)]
10. Sato, Y.; Takikawa, T.; Takishima, S.; Masuoka, H. Solubilities and Diffusion Coefficients of Carbon Dioxide in Poly (Vinyl Acetate) and Polystyrene. *J. Supercrit. Fluids* **2001**, *19*, 187–198. [[CrossRef](#)]
11. Perry, R.H.; Green, D.W. *Perry's Chemical Engineers' Handbook*, 8th ed.; The McGraw-Hill Companies, Inc.: New York, NY, USA, 2008; ISBN 9780071422949.
12. Sanchez, I.C.; Lacombe, R.H. Statistical Thermodynamics of Polymer Solutions. *Stat. Thermodyn. Polym. Solut.* **1978**, *11*, 1145–1156. [[CrossRef](#)]
13. Park, H.; Park, C.B.; Tzoganakis, C.; Tan, K.H.; Chen, P. Surface Tension Measurement of Polystyrene Melts in Supercritical Carbon Dioxide. *Ind. Eng. Chem. Res.* **2006**, *45*, 1650–1658. [[CrossRef](#)]
14. Liu, C.; Wang, J.; He, J. Rheological and Thermal Properties of M-LLDPE Blends with m-HDPE and LDPE. *Polymer* **2002**, *43*, 3811–3818. [[CrossRef](#)]
15. von Konigslow, K.; Park, C.B.; Thompson, R.B. Application of a Constant Hole Volume Sanchez-Lacombe Equation of State to Mixtures Relevant to Polymeric Foaming. *Soft Matter* **2018**, *14*, 4603–4614. [[CrossRef](#)]
16. Sanchez, I.C.; Lacombe, R. An Elementary Molecular Theory of Classical Fluids. Pure Fluids. *J. Phys. Chem.* **1976**, *80*, 2352–2362. [[CrossRef](#)]
17. Nalawade, S.P.; Picchioni, F.; Janssen, L.P.B.M. Supercritical Carbon Dioxide as a Green Solvent for Processing Polymer Melts: Processing Aspects and Applications. *Prog. Polym. Sci.* **2006**, *31*, 19–43. [[CrossRef](#)]
18. Paterson, R.; Yampol'skii, Y.; Fogg, P.G.T.; Bokarev, A.; Bondar, V.; Ilinich, O.; Shishatskii, S. IUPAC-NIST Solubility Data Series 70. Solubility of Gases in Glassy Polymers. *J. Phys. Chem. Ref. Data* **1999**, *28*, 1255–1264. [[CrossRef](#)]
19. Sato, Y.; Yurugi, M.; Fujiwara, K.; Takishima, S.; Masuoka, H. Solubilities of Carbon Dioxide and Nitrogen in Polystyrene under High Temperature and Pressure. *Fluid Phase Equilibria* **1996**, *125*, 129–138. [[CrossRef](#)]
20. Sato, Y.; Fujiwara, K.; Takikawa, T.; Takishima, S.; Masuoka, H. Solubilities and Diffusion Coefficients of Carbon Dioxide and Nitrogen in Polypropylene, High-Density Polyethylene, and Polystyrene under High Pressures and Temperatures. *Fluid Phase Equilibria* **1999**, *162*, 261–276. [[CrossRef](#)]
21. Peng, D.Y.; Robinson, D.B. A New Two-Constant Equation of State. *Ind. Eng. Chem. Fundam.* **1976**, *15*, 59–64. [[CrossRef](#)]
22. Mark, J.E. *Physical Properties of Polymers Handbook*, 2nd ed.; Mark, J.E., Ed.; Springer: Woodbury, NY, USA, 1996; ISBN 9780387312354.
23. Höcker, H.; Blake, G.J.; Flory, P.J. Equation-of-State Parameters for Polystyrene. *Trans. Faraday Soc.* **1971**, *67*, 2251–2257. [[CrossRef](#)]
24. Orwoll, R.A. Densities, Coefficients of Thermal Expansion, and Compressibilities of Amorphous Polymers. In *Physical Properties of Polymers Handbook*; Springer: New York, NY, USA, 2007; pp. 93–101. [[CrossRef](#)]
25. Park, H.; Thompson, R.B.; Lanson, N.; Tzoganakis, C.; Park, C.B.; Chen, P. Effect of Temperature and Pressure on Surface Tension of Polystyrene in Supercritical Carbon Dioxide. *J. Phys. Chem. B* **2007**, *111*, 3859–3868. [[CrossRef](#)]
26. Gross, J.; Sadowski, G. Perturbed-Chain SAFT: An Equation of State Based on a Perturbation Theory for Chain Molecules. *Ind. Eng. Chem. Res.* **2001**, *40*, 1244–1260. [[CrossRef](#)]
27. Arce, P.; Aznar, M. Modeling of Phase Equilibrium of Binary Mixtures Composed by Polystyrene and Chlorofluorocarbons, Hydrochlorofluorocarbons, Hydrofluorocarbons and Supercritical Fluids Using Cubic and Non-Cubic Equations of State. *J. Supercrit. Fluids* **2008**, *45*, 134–145. [[CrossRef](#)]